Cancer Letters 453 (2019) 170–183

Contents lists available at ScienceDirect

Cancer Letters

journal homepage: www.elsevier.com/locate/canlet

Original Articles

The NQO1/PKLR axis promotes lymph node metastasis and breast cancer progression by modulating glycolytic reprogramming

Yang Yang[a], Guang Zhu[a], Bing Dong[a], Junjie Piao[a], Liyan Chen[a,b,**], Zhenhua Lin[a,*]

[a] Department of Pathology & Cancer Research Center, Yanbian University Medical College, Yanji, 133002, China
[b] Department of Biochemistry and Molecular Biology, Yanbian University Medical College, Yanji, 133002, China

ARTICLE INFO

Keywords:
NQO1
PKLR
Glycolytic reprogramming
Metastasis
Prognosis

ABSTRACT

Overexpression of NQO1 is associated with poor prognosis in human cancers including lung, stomach, colon, cervical, and pancreatic cancers. However, the molecular mechanisms underlying the protumorigenic capacities of NQO1 have not been fully elucidated. Here, we investigated this question and determined the molecular mechanisms underlying the roles of NQO1 in glycolysis reprogramming, proliferation, and metastasis breast cancer (BC) cells. The results indicated that NQO1 overexpression in BC cells raises glucose metabolism and metastasis related behaviors. Mechanistically, NQO1 bound to PKLR, activated the AMPK and AKT/mTOR signaling pathway and consequently induced glycolytic reprogramming. In addition, 2-deoxy-D-glucose (2-DG) or 3-bromopyruvate (3-BrPA) influenced proliferation and regulated the expression of genes involved in the epithelial-to-mesenchymal transition (EMT) by restraining glycolytic reprogramming. Finally, overexpression of NQO1 and PKLR in human BC tissues was remarkably related to lymph node (LN) metastasis and poor prognosis. Together, these results demonstrate that the NQO1/PKLR axis can promote the progression of BC by modulating glycolytic reprogramming and suggest that targeting NQO1 and its downstream effectors are promising therapeutic targets for preventing the BC progression.

1. Introduction

Cancer metastasis is a complicated multistep cellular biological process [1,2], which takes responsibility for more than 90% of cancer-relevant deaths from various solid malignancies, containing breast cancer (BC) [3]. Although encouraging progress has been made in recent years owing to the development of targeted therapy, the prognosis for BC remains poor due to invasion and metastasis [4]. Extensive studies have revealed that the primary driver of the invasion/metastasis process in BC cells is the consequence of genetic or epigenetic alterations [5]. Hence, exploration of primary molecules and mechanisms underlying BC metastasis regulation is stringent requirement.

NAD(P)H:quinone oxidoreductase-1 (NQO1), aka DT-diaphorase, is a cytoplasmic flavoenzyme encoded by a gene located on human chromosome 16q22 [6,7]. The enzyme uses nicotinamide adenine dinucleotide (NADH) or NAD phosphate (NADPH) as zymolyte to directly block quinones to hydroquinone [8,9]. In recent years, the role of NQO1 in different kinds of malignant tumors has gained widespread attention from scholars [10,11]. Ma et al. revealed that NQO1 protein expression was higher in squamous cell carcinoma tissue of the cervix than in normal cervical epithelia and was closely related to clinical stage, differentiation and lymph node metastasis [12]. Zhang et al. demonstrated that NQO1 overexpression restrains proliferation and induces apoptosis in hepatocellular carcinoma (HCC) cells by activating AMPK/PGC-1α signaling pathway [13]. Additionally, Cheng et al. demonstrated that NQO1 can potentiate non-small cell lung cancer (NSCLC) cells proliferation by enhancing glycometabolism and that NQO1 depletion triggers a metabolic shift in the tricarboxylic acid (TCA) cycle independent of pyruvate dehydrogenase complex component X (PDHX) and pyruvate dehydrogenase kinase (PDK) [14]. These studies indicated that high expression of NQO1 is associated with malignant tumor progression in multiple cancers. Our previous studies found that NQO1 can be used as an early diagnostic and prognostic indicator for BC [10], but its role and mechanism in the progression of BC remain unclear. Therefore, it is urgent to study the mechanism of NQO1 underlying the biological behavior of BC and provide an effective theoretical basis for targeted therapy for BC.

Metabolic reprogramming is one hallmark of cancer cells [15]. Even in the exposure of oxygen, cancer cells primarily rely on glycolysis, instead of oxidative phosphorylation, for adenosine triphosphate (ATP)

* Corresponding author.
** Corresponding author. Department of Pathology & Cancer Research Center, Yanbian University Medical College, Yanji, 133002, China.
E-mail addresses: lychen@ybu.edu.cn (L. Chen), zhlin720@ybu.edu.cn (Z. Lin).

https://doi.org/10.1016/j.canlet.2019.03.054
Received 14 December 2018; Received in revised form 28 March 2019; Accepted 28 March 2019

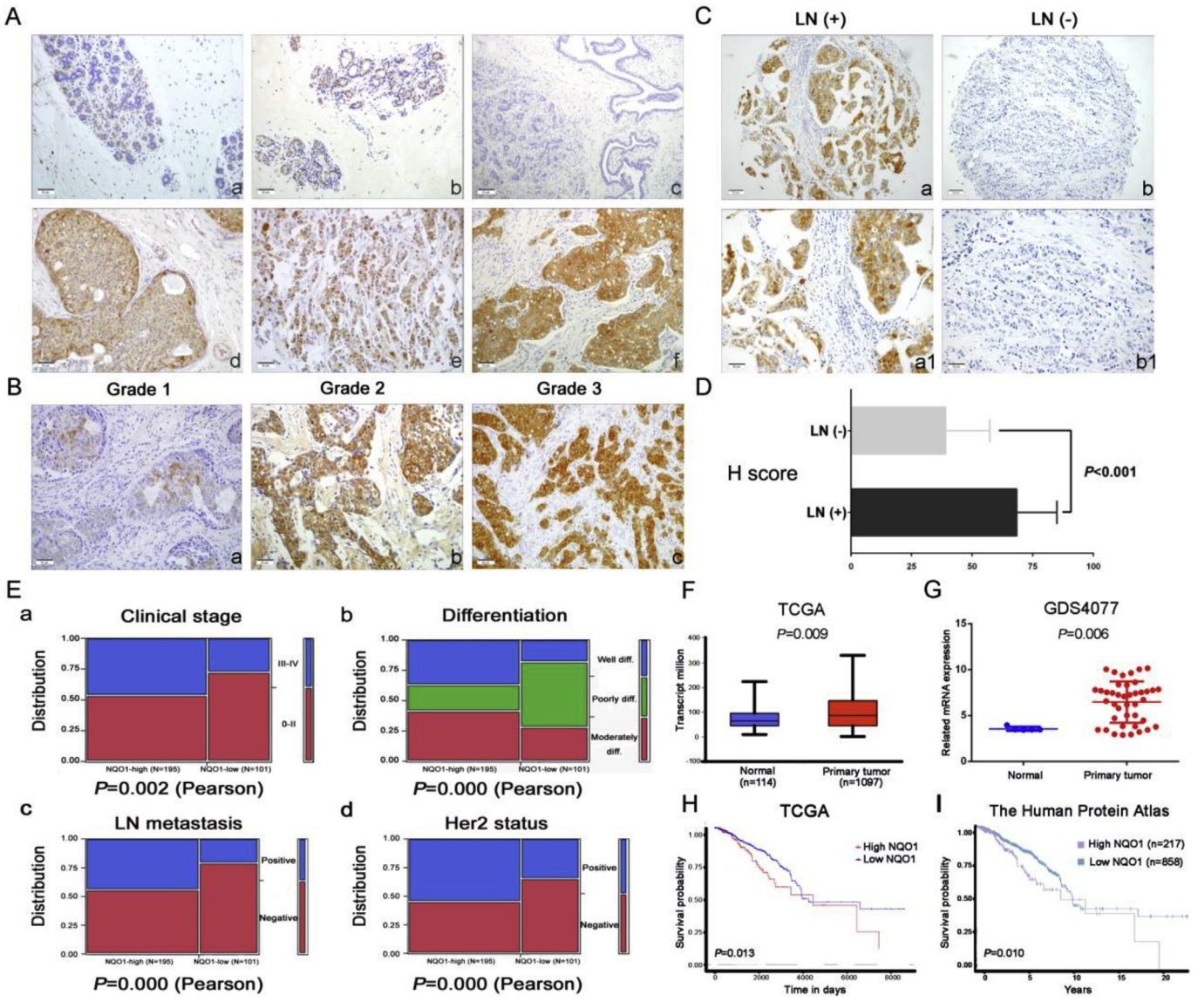

Fig. 1. Overexpression of NQO1 is closely related to LN metastasis and poor prognosis in BC. A. Representative IHC images of NQO1 expression in BC tissues and adjacent normal breast tissues (×200). B: Representative IHC images of NQO1 expression in Grade 1, 2, or 3 BC (×200). C: Representative IHC images of NQO1 expression in BC with lymph node metastasis (LN (+)) and tumors without lymph node metastasis (LN (-)) (×100, ×200). D: H-scores of NQO1 expression (mean ± SD). E: Relationships between NQO1 expression and clinicopathologically significant aspects of BC. F: Analysis of NQO1 expression levels in a TCGA data set in normal vs BC tissues ($P = 0.009$). G: Expression of NQO1 mRNA in matched adjacent normal tissues and BC tissues in the GDS4077 dataset ($P = 0.006$, Student's *t*-test). H: Correlation between NQO1 expression and overall survival in BC patients as assessed by Kaplan-Meier survival analysis (TCGA, n = 1081, $P = 0.013$). I: Correlation between NQO1 expression and overall survival in BC patients as assessed by Kaplan-Meier survival analysis (Human Protein Atlas, n = 1075, $P = 0.010$). The *P* values for the Kaplan-Meier curves were calculated using a log-rank test.

generation. The metabolic abnormity is generally referred to as the "Warburg effect" (aerobic glycolysis) and confers a proliferative advantage to cancer cells [16,17]. The pyruvate kinase family accelerates the first rigorous and irreversible step of glucose metabolism, and manipulates the magnitude and direction of glucose flux [18,19]. Pyruvate kinase, which is present in the liver and red blood cells (PKLR), is the primary isozyme of the pyruvate kinase family and exhibits significantly elevated expression in various malignancy types compared with that in normal cells. Silencing PKLR interdicts autophagosome formation in MCF-7 BC cell under optimal culture conditions [20]. Moreover, the alternative spliced isoform pyruvate kinase M2 (PKM2) conduces to the Warburg effect by accelerating aerobic glycolysis, but the PKM1 isoform affects oxidative phosphorylation [21,22]. However, despite the crucial role of pyruvate kinase in tumorigenesis, its regulatory mechanism is not adequately understood.

The current study investigated the clinicopathologic significance of NQO1/PKLR expression in a large number of BC cases via an immunohistochemical (IHC) study. Furthermore, we analyzed the effects of NQO1 overexpression on cell growth, metastasis and glycolytic reprogramming, which are thought to be fundamental to tumor progression. These findings suggest that the NQO1/PKLR axis can accelerate the progression of BC via activating AMPK and Akt/mTOR signaling pathway, which provides potential targets for future BC treatments.

2. Materials and methods

2.1. Ethics statement

This study complied with the principles of the Declaration of

Helsinki and was approved by the human ethics and research ethics committees of Yanbian University Medical College in China. All patients whose tissues used in this research were provided written informed consent. Their resected specimens were stored by our hospital and will potentially be used for scientific research. Their privacy will be maintained.

2.2. Clinical samples

The study of 296 paraffin embedded BC samples, 77 DCIS samples, 95 adjacent non-tumor tissues were conducted. These samples were selected randomly from patients who underwent surgery between 2002 and 2009, with strict follow-up for survival status. Clinicopathological classification and staging were determined according to the American Joint Committee on Cancer (AJCC) criteria.

2.3. Cell culture

The human BC cell lines MCF-7, Hs-578T, MDA-MB-231, MDA-MB-468, MDA-MB-453 and SK-BR-3 were cultured-in Dulbecco's Modified Eagle Medium (DMEM) containing 10% fetal bovine serum (FBS) and streptomycin-penicillin (100 U/mL). Cells were incubated at 37 °C in an atmosphere of 5% CO_2.

2.4. Antibodies

Antibodies against ZO-1, E-cadherin, Vimentin, Snail, Slug, Twist, p-S6, S6, p-Akt, Akt, p-4EBP-1, 4EBP-1, PKM2 and β-Actin were purchased from Cell Signaling Technology (Boston, USA). Antibody against G6PC, HOOK3, PKLR, AMPK and p-AMPK were purchased from Proteintech (Wuhan, China). NQO1 was purchased from Santa Cruz Biotechnology (CA, USA). MMP-2 was purchased from Affinity (Cincinnati, USA).

2.5. Transfection

We purchased three different PKLR siRNA, including si-RNA1, si-RNA2, and si-RNA3, from RIBOBIO (China). According to the KD effect, si-RNA1 and si-RNA2 were used in this study. The sequence of si-RNA1 (si-PKLR 1) was 5′-CAGACACCTTCCTGGAACA-3′; si-RNA2 (si-PKLR 2) was 5′-GTGCAATTTGGCATTGAAA-3′. Additionally, control siRNA (si-control) was also used in this study. Cells were transfected with 30 nM siRNA using Lipofectamine 3000 (Invitrogen) according to the manufacturer's instructions.

2.6. Stable cell line generation

Human Lenti-shNQO1-GFP, Lenti-NQO1-GFP and their controls (Lentivector control and Lenti-shSCR) were packaged in HEK293T cells. For stableinfection, 6×10^4 cells were plated in six-well plates. Following lentiviral infection, single-cell clonal isolates were selected in the presence of 2 μg/mL puromycin for 2 weeks to establish stable-expression cell lines. Transfection efficiency was confirmed by Western blot (Fig. 2B).

2.7. Wound healing assay

Cells were plated into six-well plates at 95% confluence in complete tissue culture medium. After the cells became confluent, cell wounds were created by scratching cells using a micropipette tip. The medium was then immediately replaced, and spontaneous cell migration was monitored using a Nikon inverted microscope at 0 h, 24 h and 48 h. The distance of wound closure was measured in three independent wound sites per group. The wound gaps were measured at each time.

2.8. Immunofluorescence

Cells grown in six-well culture slides fixed with 4% paraformaldehyde for 15 min, permeabilized with 0.5% Triton X-100 (CWBIO, China) and blocked with 3% BSA for 2 h. Cells were incubated with primary antibody in 3% BSA at 4 °C overnight, washed three times with PBS, incubated with Alexa Fluor 488 or Alexa Fluor 546-labeled secondary antibody (Invitrogen) in 3% BSA for 2 h, and then analyzed by Leica SP5II confocal microscope.

2.9. Cell invasion and migration assays

Cell invasion and migration assays were performed in 24-well, two-chamber plates with high-throughput screening multiwell inserts (BD Biosciences, San Jose, CA, USA), which contained 8-μm (pore size) polycarbonate filters. For cell invasion, 5×10^4 cells were added to the upper chamber, medium with fibronectin (20 μg/mL) was added to the lower chamber, and the cells were incubated at 37 °C for hours. For cell migration, 3×10^4 cells were added to the upper chamber, medium without fibronectin was added to the lower chamber, and the cells were incubated at 37 °C for hours. Invaded or migrated cells (on the lower side of the membranes or in the lower well) were then fixed in 100% methanol for 30 min and stained with gentian violet solution for 10 min. Cells were counted under a microscope at ×200 magnification. Each assay was performed in duplicate and repeated three times.

2.10. MTT and colony formation assays

The cells were seeded at a concentration of 1×10^4 cells per well in 96-well plates. After 48-h incubation with 5-AdC, the medium was removed and replaced with 100 μL per well of fresh medium containing 20 μL of MTT reagent (5 mg/mL) and incubated for 4 h at 37 °C. Then 100 μL of dimethyl sulfoxide was added, and the optical density was measured at 550 nm using an ELISA plate reader.

2.11. EdU assay

Cell proliferation was determined by 5-ethynyl- 2′-deoxyuridine (EdU) incorporation assay, which was carried out using Cell-Light™ EdU Apollo®488 In Vitro Imaging Kit (RiboBio) according to the manufacturer's instructions and analyzed by Leica SP5II confocal microscope.

2.12. Western blot

Immuno-blot analysis was performed as previously described [23]. Cells were collected and lysed with protease inhibitors. Equal amounts of proteins was loaded on SDS-PAGE gels and then transferred to a PVDF membrane (Millipore). After blocking with 5% non-fat milk, the membrane was incubated overnight at 4 °C with the primary antibody and then with horseradish peroxydase-coupled secondary antibody (Millipore). Signal was detected with enhanced chemiluminescence (Millipore).

2.13. Immunohistochemistry

IHC analysis was performed using the DAKO LSAB kit (DAKO A/S, Glostrup, Denmark). Briefly, tissue sections were deparaffinized, rehydrated and incubated with 3% H_2O_2 in methanol for 15 min at RT. The antigen was retrieved at 95 °C for 20 min using a 0.01 M sodium citrate buffer (pH 6.0). The slides were then incubated with the primary antibody at 4 °C overnight. After incubation with the secondary antibody at RT for 1 h, immunostaining was developed using DAB, and the slides were counterstained with hematoxylin.

Two pathologists (Lin Z & Piao J) who did not possess knowledge of the clinical data examined and scored all tissue specimens. In case of

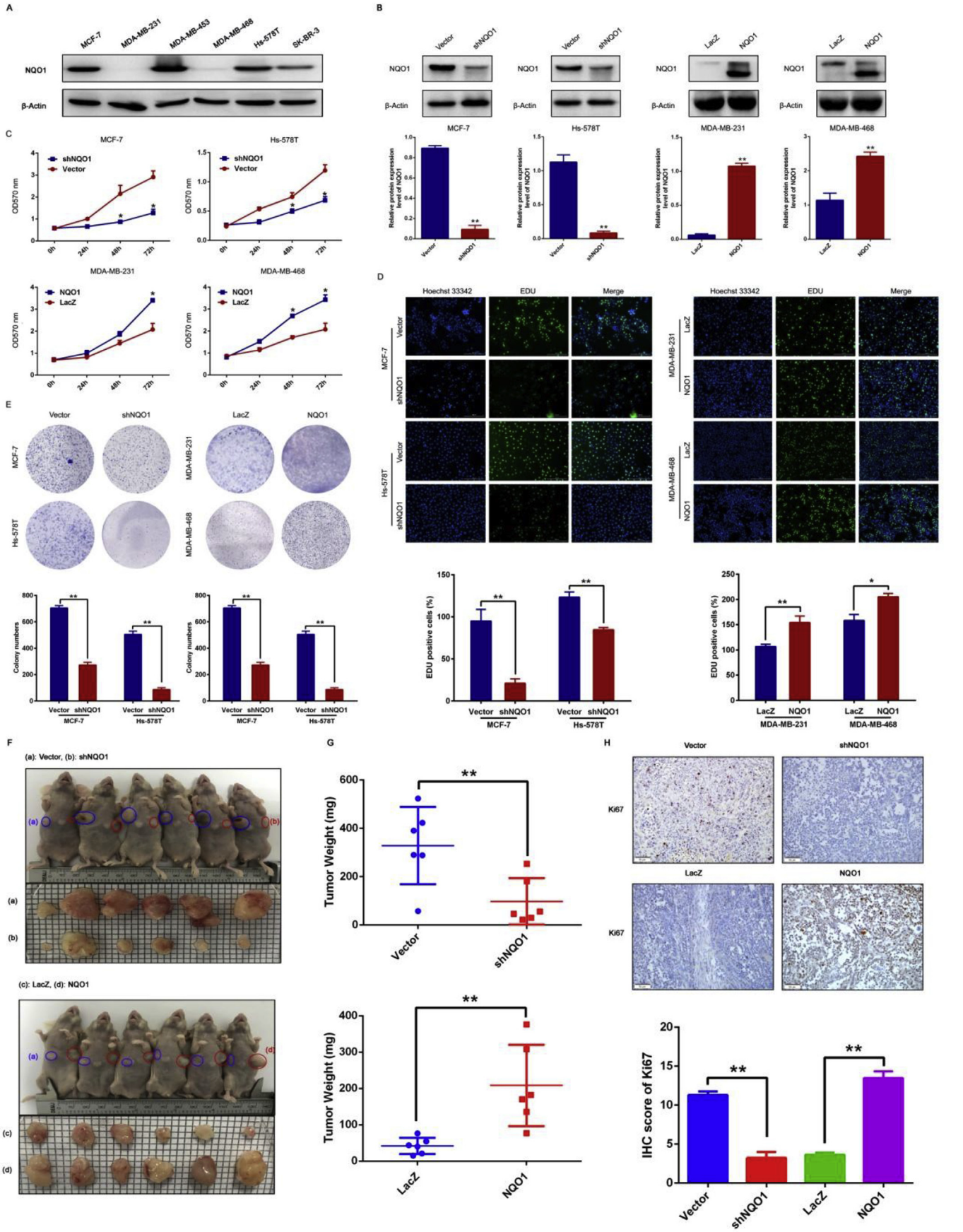

(caption on next page)

Fig. 2. NQO1 influences BC cell growth. A: Protein expression levels of NQO1 in BC cell lines as determined by Western blot analysis. B: MCF-7/Hs-578T cells with NQO1 silencing and MDA-MB-231/MDA-MB-468 cells with NQO1 overexpression were established by viral transduction. The NQO1 levels in these established cell lines were verified by Western blot analysis at 48 h after transfection. C: Cell viability was examined by MTT assay. D: Results of EdU assays on BC cells. Representative photographs are shown at the original magnification, ×100. E: Survival was measured by clonogenic assay. F: Images of mice with tumors formed by injecting the indicated cells. G: The tumor weight curves are summarized in the line chart (*$P < 0.05$ and **$P < 0.01$). H: IHC staining of the proliferation marker Ki67 in xenograft tumors. The percentage of Ki67-positive cells is summarized in the bar chart. The *P* values were obtained using Mann-Whitney *U* tests or *t*-tests (*$P < 0.05$, **$P < 0.01$). All results are from three independent experiments. The error bars represent the SD.

Table 1
NQO1 expression in BC.

Diagnosis	No. of cases	Positive cases				Positive cases rates	Strongly positive rates
		–	+	++	+++		
Breast cancers	296	43	58	113	82	85.5%**	65.9%**
DCIS	77	35	16	19	7	54.5%*	33.8%*
Adjacent non-tumor	95	69	16	10	0	27.4%	10.5%

*$P < 0.05$ and **$P < 0.01$: compared with adjacent non-tumor.
DCIS: ductal carcinoma in situ.

Table 2
Correlation between NQO1 protein expression and the clinicopathological parameters of BC.

Variables	No. of cases	NQO1 strongly positive cases (%)	χ^2	*P* value
Age			1.127	0.288
≥50	152	101 (66.4%)		
< 50	144	94 (65.3%)		
Menopausal status			3.752	0.053
premenopausal	118	70 (59.3%)		
Postmenopausal	178	125 (70.2%)		
Tumor size			0.993	0.319
T1	132	91 (68.9%)		
T2	164	104 (63.4%)		
Histological grade			18.605	0.000**
Grade-1	99	40 (40.4%)		
Grade-2	108	77 (71.3%)		
Grade-3	89	69 (77.5%)		
Clinical stage			9.429	0.002**
0-II	178	105 (59.0%)		
III-IV	118	90 (76.3%)		
LN metastasis			9.779	0.002**
Yes	107	77 (72.0%)		
No	189	101 (53.4%)		
ER			0.582	0.446
Positive	176	119 (67.6%)		
Negative	120	76 (63.3%)		
PR			0.456	0.499
Positive	137	93 (67.9%)		
Negative	159	102 (64.2%)		
Her2 status			18.742	0.000**
Positive	142	107 (75.4%)		
Negative	154	88 (57.1%)		

**$p < 0.01$.

discrepancies, a final score was established by reassessment by both pathologists on a double-headed microscope. Briefly, the IHC staining for NQO1, PKLR, HOOK3, G6PC, PKM2, E-cadherin, Vimentin and Ki67 were semi-quantitatively scored as '–' (negative) (no or less than 5% positive cells), '+' (5–25% positive cells), '++' (26–50% positive cells) and '+++' (more than 50% positive cells). The cytoplasmic expression pattern was considered as positive staining. Tissue sections scored as '++' and '+++' were considered as strong positives (overexpression) of NQO1, PKLR, HOOK3, G6PC, PKM2, E-cadherin, Vimentin and Ki67 protein.

2.14. Measurement of glucose, lactate, and ATP

The media from cultured cells were used for measuring glucose and lactate by a FlexBioanalyzer (NOVA Biomedical). Amounts of glucose remained in the cell culture medium reflected the subtraction of the consumption by cells from total glucose level in uncultured medium. ATP levels were measured using Bioluminescence Assay Kit CLS II from Roche Scientific (Indianapolis, IN, USA), as per the manufacturer's protocol. Cell lysates were used for the determination. Measurements of the metabolites were normalized to cell number.

2.15. ROS and measurement of NADPH

Cells were transfected with indicated expression vectors as described above, then the same number of the cells were re-seeded to 24 well-plates. Intracellular ROS level was stained using CellROX Green Reagent (Life Technologies, Carlsbad). Images were taken with DMI6000B (Leica, Heidelberg, Germany) and analyzed using ImageJ software. The results were expressed as the mean fluorescence intensity per cell. The intracellular levels of NADPH and total NADP were measured with the NADP/NADPH-Glo Kit (Promega, cat. no. G9081) according to the manufacturer's instructions.

2.16. Co-immunoprecipitation

MCF-7 and Hs-578T cells were lysed with RIPA Cell Lysis buffer (Beyotime). Lysates were incubated with the anti-NQO1 antibody (Santa Cruz Biotechnology) or the anti-PKLR antibody (Proteintech) in presence of protein A/G agarose beads (Santa Cruz Biotechnology) overnight at 4 °C. Beads were centrifuged at 4000 r.p.m. for 30 s and washed with cold RIPA lysis buffer. Proteins were resolved by SDS-PAGE, transferred to membranes, and analyzed by western blotting as described above.

2.17. In vivo tumorigenesis and metastasis assays

BALB/c nude mice (4–6 weeks old) were purchased from the Vital River Laboratory Animal Technology Co. Ltd., (Beijing, China). All mice were housed in specific pathogen-free conditions following the guidelines of the Institutional Animal Care. To assess the effect of NQO1 on tumorigenicity *in vivo*, Hs-578T cells (3×10^6 cells, with vector or shNQO1) and MDA-MB-231 cells (3×10^6 cells, with lacZ or NQO1) were subcutaneously injected into the left flank of the mice. Xenograft growth was monitored every week using a caliper. Tumor volume (V) was monitored by measuring the length (L) and width (W) of the tumor with calipers and was calculated with the formula $V = (L \times W^2) \times 0.5$. Immunohistochemical staining for NQO1, PKLR, Vimentin, E-cadherin, HOOK3, G6PC, PKM2, Ki67 were performed on sections from the tumors. All experiments were performed in keeping with the procedures and protocols of the Animal Ethics Committee of Yanbian University. To produce experimental metastases, Hs-578T cells (1×10^6 cells, with vector or shNQO1) and MDA-MB-231 cells (1×10^6 cells, with lacZ or NQO1) were harvested in serum-free DMEM medium and injected into the tail vein of nude mice (7 mice/group). The mice were sacrificed after 6 weeks and the lungs were surgically excised and stained with H&E. Lung metastatic lesions were evaluated under a dissecting microscope (×200 magnification).

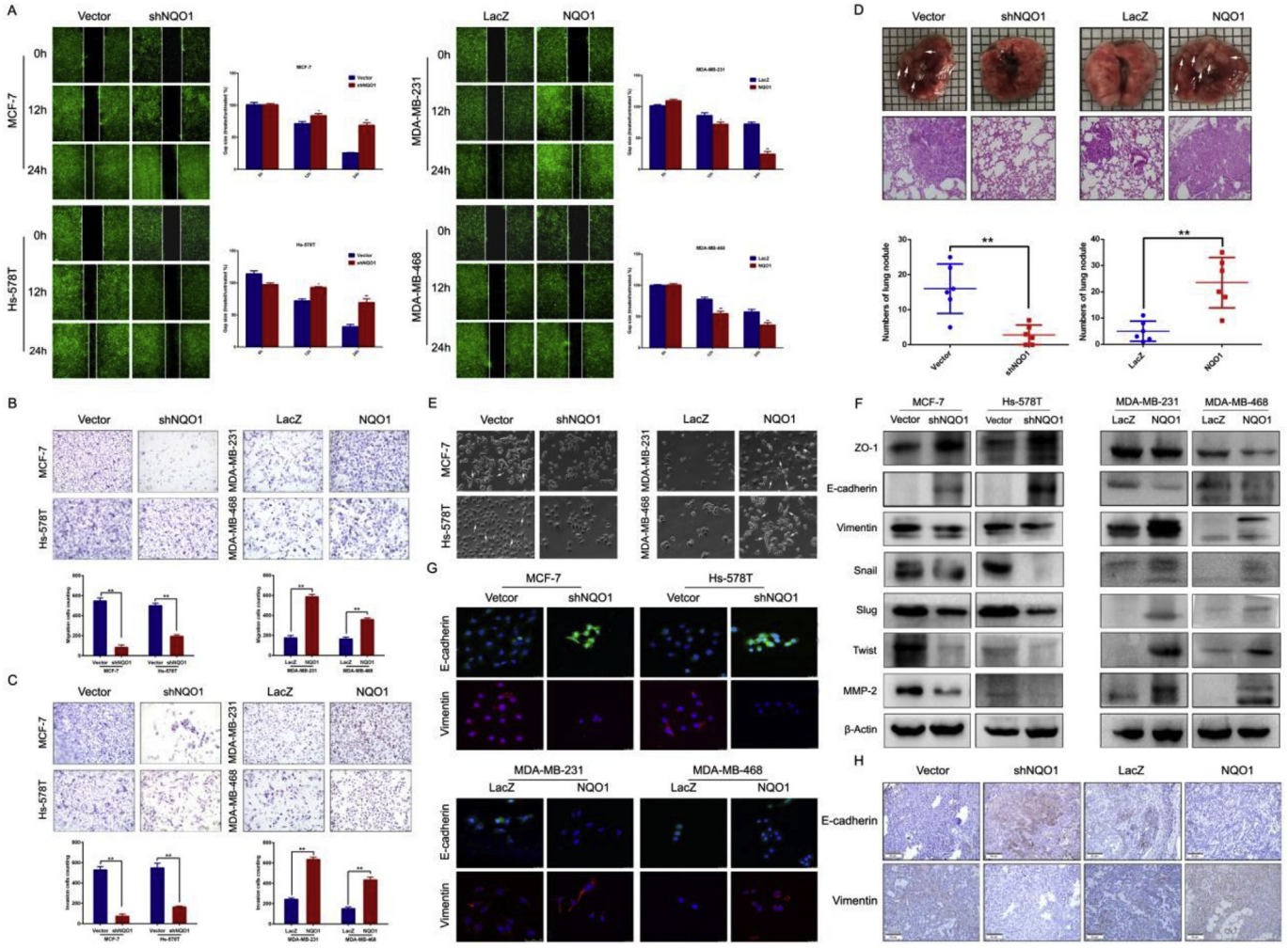

Fig. 3. NQO1 promotes cellular invasion, metastasis and the EMT *in vitro* and *in vivo*. A: A scratch wound-healing assay was used to determine the effects of NQO1 on BC cell motility. B and C: Results of a transwell migration assay (B) and a Matrigel invasion assay (C) for cellular invasion. The mean number of cells in five fields per membrane is shown (×200). D: Representative images of gross and hematoxylin and eosin (H&E) staining and the numbers of lung surface metastatic foci detected in each group (**$P < 0.01$; ×200). The scale bar is 25 μm. E: Representative images showing the morphological changes in the indicated cell lines. F: The expression of epithelial markers (E-cadherin and ZO-1) and mesenchymal markers (Vimentin, Snail, Slug, Twist and MMP-2) was determined by Western blot analysis. β-Actin was used as a loading control. G: The expression of EMT markers was detected by immunofluorescence staining in BC cells (100×). H: IHC staining for E-cadherin and Vimentin protein in tumor specimens from xenografts (200×). The *P* values were obtained using Mann-Whitney *U* tests or *t*-tests (*$P < 0.05$, **$P < 0.01$). All results are from three independent experiments. The error bars represent the SD.

2.18. Statistical analysis

The data analysis was performed using SPSS 17.0 software and GraphPad Prism 6.0 software. Associations between NQO1, PKLR expression and clinicopathological features were evaluated by a Chi-square test and Fisher's exact test. The Kaplan-Meier method was used for analysis of survival curves, and statistical significance was assessed using the Log-rank test. Group comparisons for continuous data were done by Mann-Whitney *U* Test, one-way ANOVA or Student's *t*-test. Biochemical experiments were performed in triplicate and a minimum of three independent experiments were evaluated. Spearman correlation analysis was used for ranking correlation tests. The value of $P < 0.05$ was considered statistically significant.

3. Results

3.1. NQO1 overexpression correlates with lymph node metastasis and poor prognosis in BC

To investigate the role of NQO1 in human BC, we first examined NQO1 expression in 296 pairs of BC tissues, 77 ductal carcinoma in situ (DCIS) tissues and 95 normal breast tissues by IHC. As shown in Fig. 1A, staining for NQO1 was negative in nontumor breast tissues but positive in BC tissues. IHC staining also showed that NQO1 is predominantly localized in the nucleus and cytoplasm of tumor cells. The positive staining rate of NQO1 was 85.5% (253/296) in BC tissues, which was significantly higher than that in DCIS (54.5%, 42/77) and adjacent nontumor tissues (27.4%, 26/95) ($P < 0.001$) (Table 1). Notably, NQO1 protein level was markedly up-regulated in BC tissues with Grade 2 and Grade 3 compared with Grade 1 (Fig. 1B). Moreover, NQO1 expression was detected in 72.0% (77/107) of the tissue microarray (TMA) samples and all the samples with lymph node metastases (Fig. 1C). H-scores in patients with lymph node metastasis were significantly higher than those without metastasis (Fig. 1D). As shown in Table 2, NQO1 expression was correlated with histological grade ($P = 0.000$), clinical stage ($P = 0.002$), and Her2 status ($P = 0.000$) (Fig. 1E). However, statistically significant associations were not observed between NQO1 expression and age ($P = 0.288$), menopausal status ($P = 0.053$), tumor size ($P = 0.319$), ER status ($P = 0.446$) or PR status ($P = 0.499$).

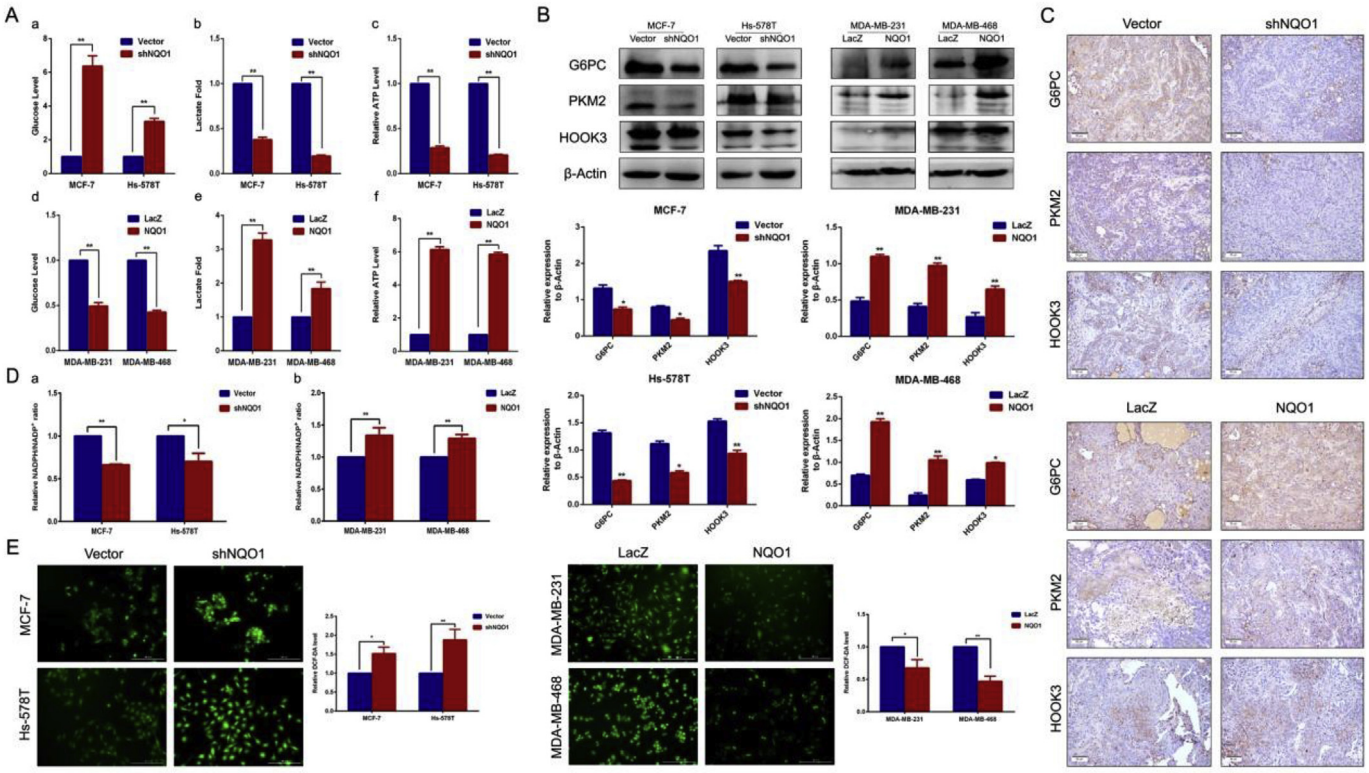

Fig. 4. NQO1 supports increased glycolysis by NADPH homeostasis. A: Overexpression of NQO1 promotes aerobic glycolysis. Cell culture media were collected to measure glucose (a and d), lactate (b and e) and cellular ATP (c and f) levels were measured. The metabolite levels were normalized to the number of cells. The value in the control group was set as "1". The means ± SD for 3 independent experiments are presented (**$P < 0.01$). B: The expression of metabolic enzymes (G6PC, PKM2 and HOOK3) was determined by Western blot analysis. β-Actin was used as a loading control. C: IHC staining for G6PC, PKM2 and HOOK3 protein in tumor specimens from xenografts (200×). D and E: NADPH/$NADP^+$ (D) or intracellular ROS (E) levels in the indicated cells cultured in attached or detached conditions. The means ± SD for 3 independent experiments are presented (**$P < 0.01$). The P values were obtained using Mann-Whitney U tests or t-tests (*$P < 0.05$, **$P < 0.01$). All results are from three independent experiments. The error bars represent the SD.

We further analysis the mRNA expression of NQO1 in BC from the Cancer Genome Atlas (TCGA), and discovered that NQO1 mRNA levels were significantly up-regulated in BC tissues ($P = 0.009$, Fig. 1F). Similarly, overexpression of NQO1 in BC samples was identified in the GDS4077 dataset ($P = 0.006$, Fig. 1G). Importantly, the TCGA cohort and the Human Protein Atlas showed that BC patients with high NQO1 expression had obvious shorter survival time than those in low NQO1 group (Fig. 1H: $P = 0.013$; Fig. 1I: $P = 0.010$). Overall, these results indicate that high expression of NQO1 is well correlates with metastasis and poor prognosis in BC patients.

3.2. NQO1 enhances tumorigenesis in vitro and in vivo

To determine the biological functions of NQO1 in BC, we first examined NQO1 expression in immortalized benign human mammary epithelial MCF-10A cells and a series of BC cell lines (MCF-7, MDA-MB-231, MDA-MB-453, MDA-MB-468, Hs-578T, and SK-BR-3) by Western blot analysis. Among the six BC cell lines, NQO1 displayed the highest expression levels in MCF-7 and Hs-578T cells and the lowest expression levels in MDA-MB-231 and MDA-MB-468 cells (Fig. 2A). Therefore, we established stable overexpression of NQO1 (designated NQO1) in MDA-MB-231 and MDA-MB-468 cells and stable knockdown of NQO1 (designated shNQO1) in MCF-7 and Hs-578T cells. Western blot was performed to measure the protein levels of NQO1 expression (Fig. 2B). MTT and EdU assays revealed that NQO1 knockdown markedly inhibited cell proliferation and the percentage of EdU-positive cells (Fig. 2C and D), whereas NQO1 overexpression enhanced cell proliferation and the percentage of EdU-positive cells. Additionally, a clonogenic assay demonstrated that silencing NQO1 resulted in considerably fewer and smaller colonies, whereas NQO1 overexpression enhanced clonogenicity (Fig. 2E).

In order to verify the results *in vitro*, we investigated the effects of NQO1 on tumorigenesis using xenograft mouse model. As shown in Fig. 2F and G, the average volume and weight of tumors in the shNQO1 group were markedly decreased in comparison with the control group. Moreover, IHC staining showed that the shNQO1 group had lower Ki67 proliferation indexes than in the control group (Fig. 2H). The result was further confirmed in NQO1 overexpressed group. Together, these results indicate that NQO1 can regulate the proliferation process of BC.

3.3. NQO1 induces the EMT and promotes cellular migration and invasion

The aforementioned results suggest that NQO1 was associated with BC metastasis. To further explore the effects of NQO1 on metastatic ability of BC, *in vitro* and *in vivo* assays were performed. As shown in Fig. 3A–C, wound-healing and transwell assays demonstrated that cell migration and invasion were markedly increased in NQO1 cells but were decreased in shNQO1 cells, compared to the corresponding control cells. Furthermore, to test the *in vivo* suppressive effect of NQO1 on metastasis, Hs-578T-vector, Hs-578T-shNQO1, MDA-MB-231-LacZ and MDA-MB-231-NQO1 cells were injected into the caudal vein of nude mice (n = 6). As shown in Fig. 3D, compared with those in the control group, mice injected with shNQO1 had fewer lung metastases. Conversely, mice injected with NQO1 had more. In summary, these results indicate that high NQO1 expression promotes BC invasion and metastasis.

It is generally known that EMT enables cancer cells acquire the ability of invasion and metastasis [24]. Interestingly, the results

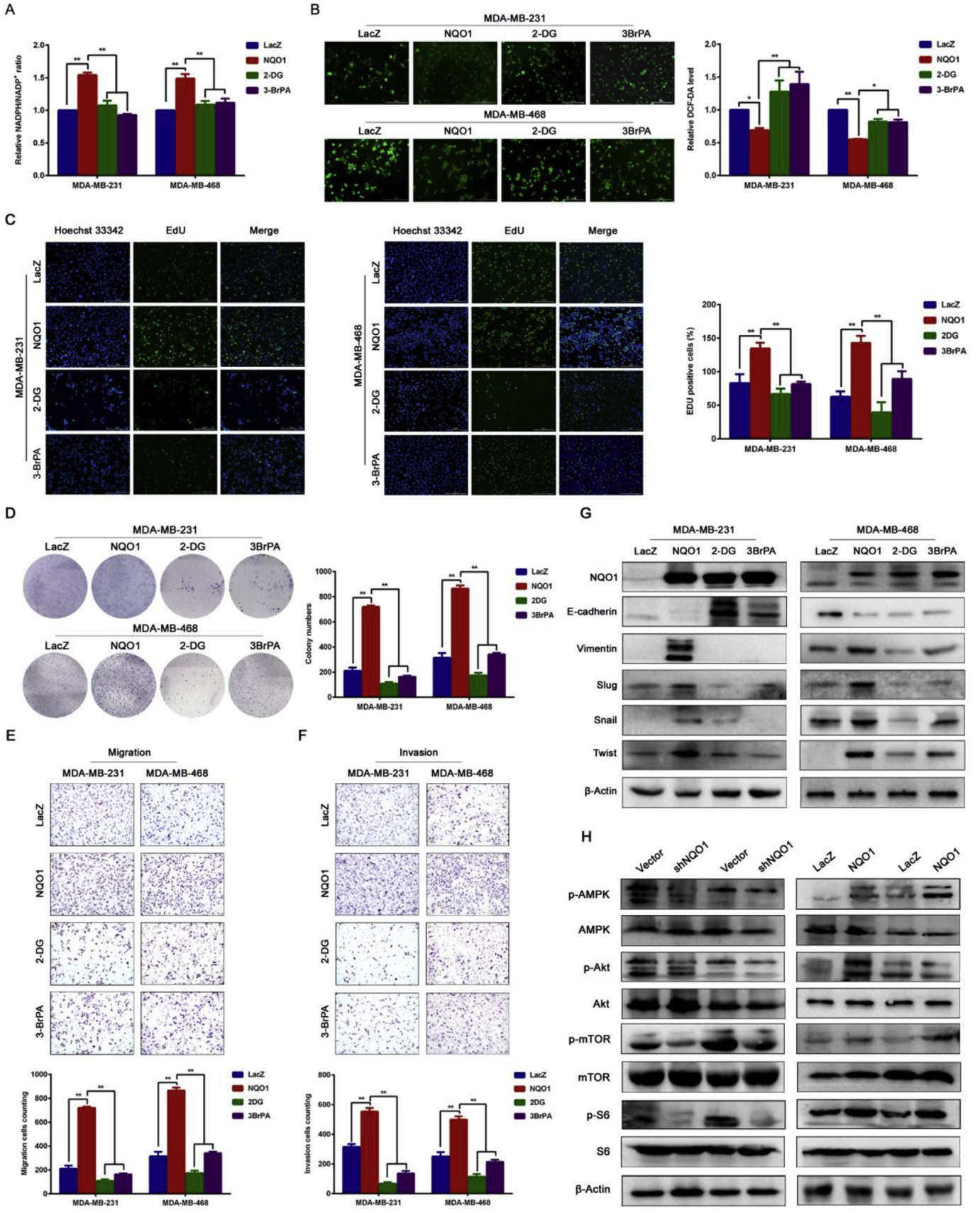

(caption on next page)

Fig. 5. NQO1 promotes BC progression by modulating aerobic glycolysis. A and B: NADPH/$NADP^+$ (A) or intracellular ROS (B) levels of indicated cells cultured in attached or detached conditions. The means ± SD for 3 independent experiments are presented (**$P < 0.01$). C: EdU assays in MDA-MB-231 and MDA-MB-468 cells overexpressing NQO1 and treated with 2-DG or 3-BrPA. Representative photographs of the EdU assays are shown at the original magnification, (×100). D: Representative images showing the colony formation ability of MDA-MB-231 and MDA-MB-468 cells overexpressing NQO1 and treated with 2-DG or 3-BrPA after 2 weeks of seeding (×100). E and F: For migration and invasion assays, NQO1 cells were cultured in a Boyden chamber and treated with 2-DG or 3-BrPA. After 24 and 48 h, the cells were fixed and stained with crystal violet. Stained cells on the bottom membrane were counted in five microscopic fields per sample (×200). G: Western blots of NQO1 cells overexpressing NQO1 and treated with 2-DG or 3-BrPA. The results demonstrated a reduction in the levels of EMT protein markers. H: Relative expression levels of AMPK, phosphorylated AMPK, AKT, phosphorylated AKT, mTOR, phosphorylated mTOR, S6, phosphorylated S6, and EMT markers in BC cells. The *P* values were obtained using Mann-Whitney *U* tests or *t*-tests (*$P < 0.05$, **$P < 0.01$). All results are from three independent experiments. The error bars represent the SD.

indicated that shNQO1 cells attained an epithelial morphology, while NQO1 cells acquired a dispersed, spindle-shaped morphology (Fig. 3E). We detected increased levels of epithelial markers (ZO-1 and E-cadherin) and decreased levels of mesenchymal markers (Vimentin, Snail, Slug and Twist) in shNQO1 cells. Conversely, the opposite effect was shown in NQO1 cells (Fig. 3F and G). In agreement with the results *in vitro*, IHC staining of the subcutaneous tumor indicated that E-cadherin expression was increased while Vimentin expression was decreased in shNQO1 group, and overexpressing NQO1 induced the opposite results (Fig. 3H). Taken together, these results indicate that NQO1 plays important roles in BC invasion and metastasis.

3.4. NQO1 supports increased glycolysis by NADPH homeostasis

It is well accepted that tumor formation and progression require a transformation of glucose metabolism. Under the stress associated with such processes, cancer cells rely on glycolysis to fuel their malignant properties [25]. We explored whether NQO1 plays a role in glycolysis of BC. As expected, glucose uptake, lactate secretion, and ATP levels were markedly increased in NQO1 cells but were conversely decreased in shNQO1 cells (Fig. 4A). Consistent with these observations, glycolytic enzymes, including HK3, G6PC and PKM2, were upregulated in BC cells with NQO1 overexpression but downregulated with NQO1 knockdown (Fig. 4B). To provide further evidence, we measured the expression of these glycolytic metabolic enzymes in BC cell tumor xenografts using IHC staining and obtained consistent results (Fig. 4C). Thus, we conclude that NQO1 promotes the reprogramming of glycolytic metabolism in BC by affecting the expression of related metabolic enzymes.

Increasing evidence indicates the importance of NADPH homeostasis in the survival of cancer cells under conditions of metabolic stress, such as during metabolic resource limitation and therapeutic intervention [26]. To further substantiate the necessity of NQO1 in NADPH generation and glucose metabolism, we evaluated the effect of NQO1 knockdown or overexpression on cellular NADPH and glycolytic activity. The data showed that the cellular NADPH level, which was significantly increased by NQO1 silencing, was clearly restored when NQO1 was overexpressed (Fig. 4D). NADPH is a key factor in suppressing intracellular reactive oxygen species (ROS) and enhancing ATP generation [27,28]. Consistent with the trend shown for NADPH, NQO1 silencing robustly increased intracellular ROS, which could be decreased by NQO1 overexpression (Fig. 4E). These findings unequivocally demonstrate that NQO1 plays an essential role in maintaining high glycolytic activity in BC cells by supplying NADPH homeostasis.

3.5. NQO1 promotes BC cell growth and metastasis via regulating glycolytic reprogramming

Aberrant cancer metabolism plays important roles in the migration, invasion, and metastasis of cancer by regulating the EMT [29,30]. Therefore, we evaluated whether the effects of NQO1 on proliferation, metastasis and the EMT were dependent on the glycolytic pathway. NQO1 cells were treated with the glycolytic inhibitors 2-deoxy-D-glucose (2-DG) or 3-bromopyruvate (3-BrPA) for 24 h. We observed that 2-DG or 3-BrPA significantly increased intracellular ROS and decreased NADPH levels in NQO1 cells in comparison with control cells (Fig. 5A and B). In addition, inhibition of glycolysis markedly inhibited cell proliferation as determined by 5-ethynyl-2′-deoxyuridine (EdU) and colony formation assays (Fig. 5C and D). Similarly, inhibition of glycolysis significantly reduced migration and invasion capacity (Fig. 5E and F). Moreover, 2-DG or 3-BrPA reversed the NQO1-induced upregulation of Vimentin, Snail, Slug, and Twist and downregulation of E-cadherin (Fig. 5G). These results indicate that NQO1 regulates cell growth, metastasis, and the EMT in a manner dependent on the glycolytic pathway.

Previous articles have reported that the AMPK and AKT/mTOR signaling pathway plays crucial roles in the EMT [31–33]. We assumed that NQO1 likely to induced tumor growth and progression in BC cells via the AMPK and AKT/mTOR pathway. We assessed the expression levels of AMPK and AKT/mTOR signaling pathway and downstream molecules by Western blot analysis. As shown, markers of the AMPK and AKT/mTOR signaling pathway, such as the levels of phosphorylated AMPK, AKT, mTOR and S6 were upregulated by overexpression of NQO1 (Fig. 5H), which suggest that NQO1 promotes glycolytic reprogramming in BC, at least in part by regulating the AMPK and AKT/mTOR signaling pathway.

3.6. Identification of PKLR as a target gene of NQO1 in BC

In order to deeply explore the mechanism of NQO1 regulates cell metastasis and glycolysis in BC, PCR arrays and bioinformatics strategies were used. Using InBio Map analysis, we found that NQO1 enrichment in cells was significantly associated with the PKLR gene (Fig. 6A). Then, according to these microarray datasets, we carried out Gene Set Enrichment Analysis. As shown in Fig. 6B, the PKLR gene was significantly enriched in NQO1-knockdown MCF-7 cells. Western blot analysis showed that overexpression of NQO1 increased PKLR expression while shNQO1 reduced it (Fig. 6C). Similarly, we revealed that NQO1 expression is relevant to PKLR status *in vivo* (Fig. 6D). We next examined the potential binding interaction between NQO1 and PKLR using coimmunoprecipitation and colocalization approaches. As shown in Fig. 6E, NQO1 was indeed pulled down by an anti-PKLR antibody in MCF-7 and Hs-578T cells, indicating close binding between NQO1 and PKLR. In accordance with the results, immunofluorescence microscopy also showed colocalization of NQO1 and PKLR in the nucleus and cytoplasm of MCF-7 and Hs-578T cells (Fig. 6F). Together, these data suggest that PKLR is a target gene of NQO1 in BC cells.

Next, we transfected siRNA-Ctrl (si-Con) or siRNAs against PKLR (si-PKLR) into NQO1-overexpressing cells to investigate the effects of PKLR on glycolytic reprogramming and metastasis mediated by NQO1 (Fig. 6G). We found that knockdown of PKLR could effectively offset the effects of NQO1 overexpression on glucose metabolism in MDA-MB-231 and MDA-MB-468 cells, as revealed by glucose uptake, lactate secretion, and ATP levels (Fig. 6H). SiRNA-PKLR influenced intracellular ROS and decreased NADPH levels (Fig. 6I and J). Furthermore, we found that PKLR siRNA eliminated the effects of NQO1 in inducing cellular proliferation (Fig. 6K) and abolished NQO1-mediated cell invasion and migration (Fig. 6L and M). In addition, G6PC, PKM2 and HK3 expression increased by PKLR knockdown was restored to basal levels by NQO1 overexpression (Fig. 6N). Strikingly, siRNA-PKLR transfection into NQO1-overexpressing cells increased E-cadherin and

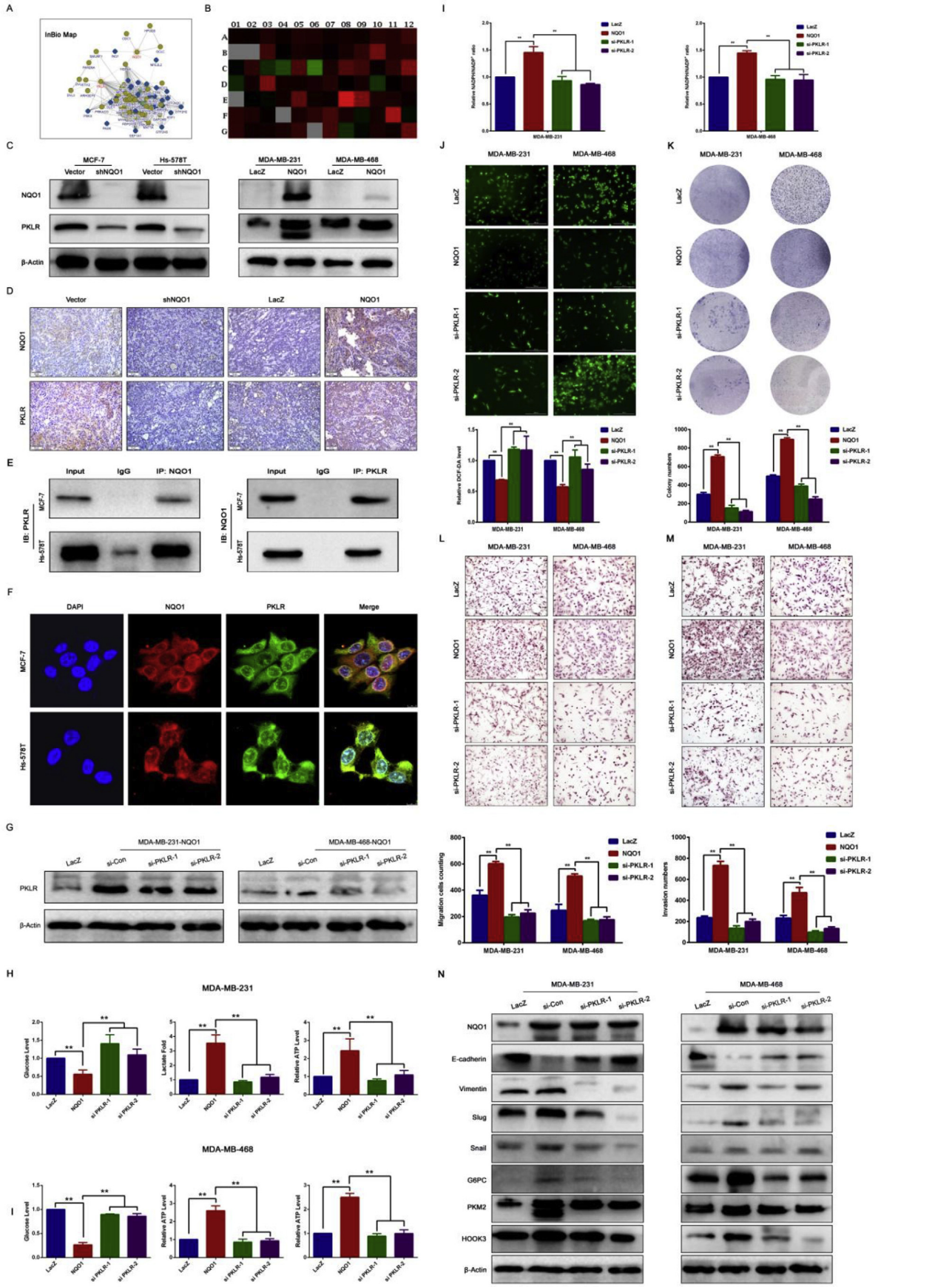

(caption on next page)

Fig. 6. Identification of PKLR as a target gene of NQO1 in BC. A: Diagram illustrating the approach used to select potential NQO1 targets for experimental validation. B: Heat maps to indicate the most differentially expressed genes in MCF-7 cells with NQO1 knockdown. The colored bands represent the expression changes for the indicated genes (green indicates downregulation, and red indicates upregulation). C: The protein expression levels of PKLR were analyzed by Western blot analysis after knockdown or overexpression of NQO1 in BC cells. D: The protein expression levels of NQO1 and PKLR were analyzed by IHC staining in tumor specimens from xenografts (200×). E: The interaction between endogenous NQO1 and PKLR protein was analyzed by coimmunoprecipitation in MCF-7 and Hs-578T cells. F: Immunofluorescence double-labeling experiments confirmed the existence of two colocalization phenomena (400×). G and H: NQO1 cells were transduced with si-Con, si-PKLR-1 or si-PKLR-2 for 48 h. The cell culture media were changed, and 24 h later, whole-cell extracts were used for immunoblots (G). Extracellular glucose and lactate and intracellular ATP (H) were measured. The metabolite levels were normalized to the number of cells. The value in the control group was set as "1". The means ± SD for 3 independent experiments are presented (**$P < 0.01$). I and J: NADPH/$NADP^+$ (I) or intracellular ROS (J) levels of the indicated cells cultured in attached or detached conditions. The means ± SD for 3 independent experiments are presented (**$P < 0.01$). K-M: MDA-MB-231 and MDA-MB-468 cells with or without NQO1 overexpression were mock-transduced or transduced with si-Con, si-PKLR-1 or si-PKLR-2 for 48 h. Cell colony formation (K), migration (L) and invasion (M) were determined. N: Western blots of NQO1-overexpressing cells treated with siRNA-PKLR-1 or siRNA-PKLR-2. The results demonstrated a reduction in the levels of EMT protein markers. The *P* values were obtained using Mann-Whitney *U* tests or *t*-tests (*$P < 0.05$, **$P < 0.01$). All results are from three independent experiments. The error bars represent the SD.

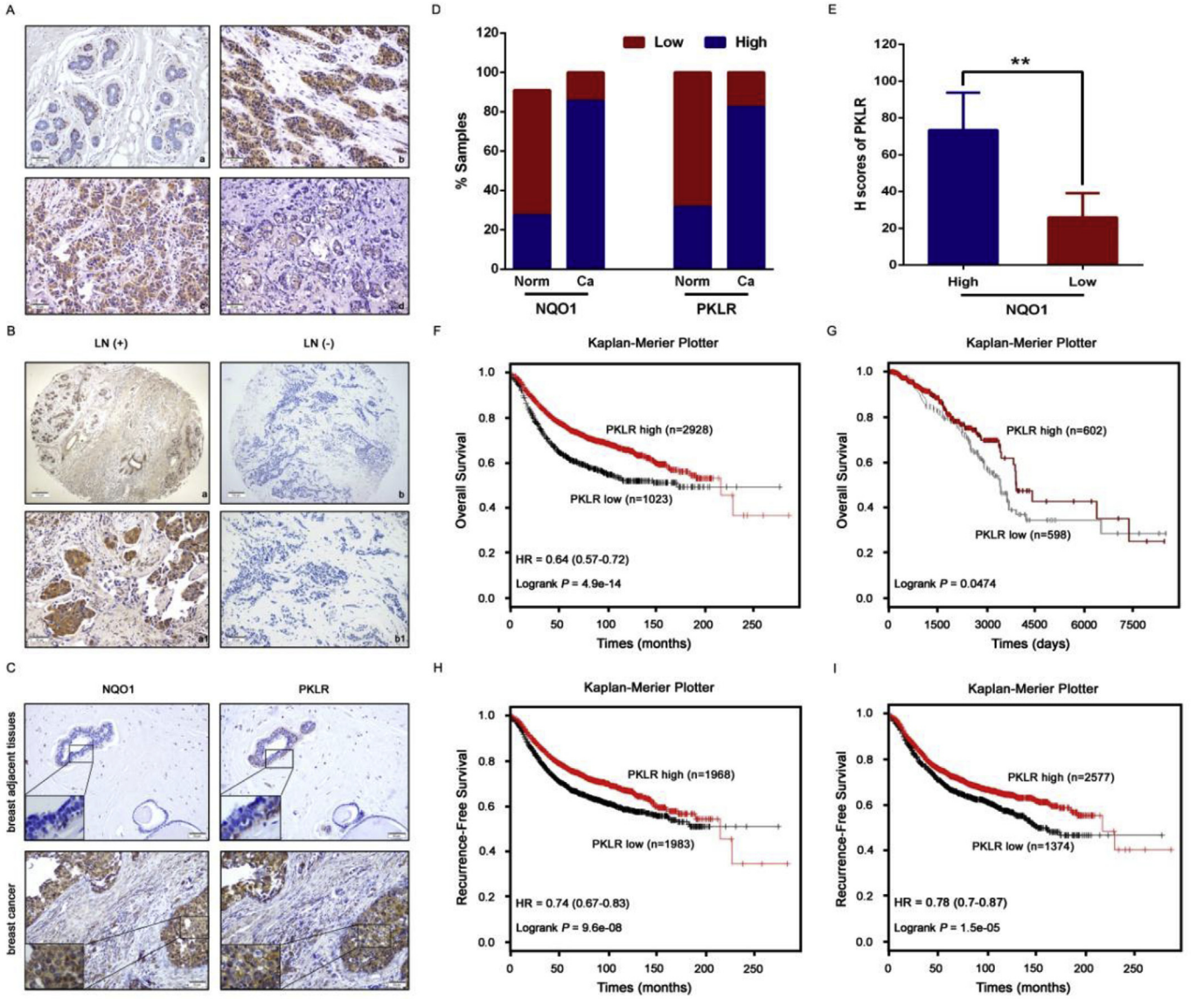

Fig. 7. High expression of NQO1 in breast tissues correlates with elevated PKLR. A. Representative IHC images of PKLR expression in adjacent normal breast tissues (a) and BC tissues (b–d) (×200). B: Representative IHC images of PKLR expression in tumor tissues with lymph node metastasis (LN (+)) and those without lymph node metastasis (LN (-)) (×100, ×200). C: Representative IHC staining of NQO1 and PKLR in normal breast tissues and in BC tissues (×200, ×400). D: Quantification of NQO1 and PKLR expression in human breast tissues (low: overall negative or weak staining; high: overall moderate or strong staining). Pearson's chi-square test was used to analyze the distribution difference of NQO1 and PKLR between healthy and BC tissues ($P < 0.01$). E: H-scores of PKLR in breast tissues with low or high levels of NQO1 (**$P < 0.01$). F and G: Overall Survival curves of patients with or without elevated PKLR levels. Patient data from a study on BC in the TCGA database were analyzed. H and I: Recurrence-Free Survival curves of patients with or without elevated PKLR levels. Patient data from a study on BC in the TCGA database were analyzed.

Table 3
PKLR expression in BC.

Diagnosis	No. of cases	Positive cases				Positive cases rates	Strongly positive rates
		–	+	++	+++		
Breast cancers	296	52	58	107	79	82.4%**	62.8%**
DCIS	77	38	14	19	6	50.6%*	32.5%*
Adjacent non-tumor	95	65	19	11	0	31.6%	11.6%

*$P < 0.05$ and **$P < 0.01$: compared with adjacent non-tumor.
DCIS: ductal carcinoma in situ.

Table 4
Correlation between PKLR protein expression and the clinicopathological parameters of BC.

Variables	No. of cases	PKLR strongly positive cases (%)	χ^2	*P* value
Age			0.358	0.550
≥50	152	98 (64.5%)		
< 50	144	88 (61.1%)		
Menopausal status			1.420	0.233
premenopausal	118	79 (66.9%)		
Postmenopausal	178	107 (60.1%)		
Tumor size			2.070	0.150
T1	132	77 (58.3%)		
T2	164	109 (66.5%)		
Histological grade			41.346	0.000**
Grade-1	99	37 (37.4%)		
Grade-2	108	81 (75.0%)		
Grade-3	89	68 (76.4%)		
Clinical stage			9.967	0.002**
0-II	178	99 (55.6%)		
III-IV	118	87 (73.7%)		
LN metastasis			11.874	0.001**
Yes	107	81 (75.7%)		
No	189	105 (55.6%)		
ER			2.680	0.102
Positive	176	110 (62.5%)		
Negative	120	86 (71.7%)		
PR			0.000	0.983
Positive	137	86 (62.8%)		
Negative	159	100 (62.9%)		
Her2 status			12.646	0.000**
Positive	142	104 (73.2%)		
Negative	154	82(53.2%)		

**$p < 0.01$.

Table 5
Association of NQO1 and PKLR expressions in BC by IHC.

PKLR expression	NQO1 expression				No. of cases	r	*P* value
	–	+	++	+++			
-	40	9	3	0	52	0.893	0.000
+	2	47	3	6	58		
++	1	2	100	4	107		
+++	0	0	7	72	79		
No. of cases	43	58	113	82	296		

decreased Vimentin, Slug and Snail expression, which reversed the NQO1-stimulated mesenchymal cell phenotype (Fig. 6N). These observations suggest that PKLR knockdown can partially reverse the biological behaviors induced by NQO1 in BC cells.

3.7. PKLR is positively correlated with the expression of NQO1 and lymph node metastasis in BC patients

To determine the clinical significance of the experimental results described above, we examined the relationship between the expression of NQO1 and PKLR and the lymph node metastasis in BC tissues by performing IHC. Tellingly, 244/296 (82.4%) of the primary tumor samples showed positive PKLR expression, while more than 75.7% (81/107) of the metastatic lymph node lesions were positive for PKLR expression (Fig. 7A and B, Tables 3 and 4). Healthy breast tissues generally displayed low NQO1 signals with little or no PKLR signals (Fig. 7C). In contrast to healthy tissues, nearly 90% of BC tissues exhibited increased expression of NQO1, and approximately 80% of BC cases were positive for PKLR (Fig. 7D). The H-scores also demonstrated intense PKLR signals in cancerous tissues with high NQO1 expression (Fig. 7E). In addition, by analyzing consecutive BC sections, we found that PKLR expression was significantly associated with NQO1 expression ($P = 0.000$, Table 5). The clinicopathological analysis revealed that PKLR expression was closely correlated with histological grade ($P = 0.000$), clinical stage ($P = 0.002$), LN metastasis ($P = 0.001$) and Her2 status ($P = 0.000$). Importantly, patients with upregulated PKLR had a significantly shorter survival period than those with normal PKLR expression ($P < 0.000$) (Fig. 7F–I). Taken together, these results indicate that the NQO1/PKLR axis is activated in primary and metastatic BC and is well correlated with poor prognosis.

4. Discussion

Over the past decades, NQO1 has been identified as a key player involved in multiple cellular events related to cancer development and has been proposed as a potential therapeutic target for cancer [34–36]. NQO1, which regulates chromatin-binding proteins and gene expression, oxidative stress, DNA damage is often aberrantly expressed in cancers [37,38]. However, the detailed mechanisms by which NQO1 is involved in aberrant metabolic remodeling and metastasis in cancer development remain largely unexplored.

Previous studies have shown that NQO1 can promote the EMT of BC cells, although the mechanism is unclear [36]. Katikireddy et al. found that NQO1 plays a vital role in mediating the EMT by activating Snail1 in postmitotic corneal cells, thus conducing to the pathogenesis of Fuchs endothelial corneal dystrophy (FECD) [39]. Consistent with the results of these studies, we revealed that several EMT markers are upregulated in NQO1-overexpressing BC cells (Fig. 3). Recently, mounting research has determined that cancer cells rewrite their metabolism to an abnormal state that favors their survival, proliferation and metastasis [40–42]. Interestingly, we found that blocking the glycolytic pathway with specific inhibitors significantly attenuated NQO1-enhanced proliferation and metastasis in BC cells. Furthermore, we delineated a molecular mechanism or cellular signaling pathway underlying the NQO1-mediated regulation of these EMT markers. In detail, we focused on pyruvate kinase family members, which are key regulatory enzymes that play important roles in various malignancies [42,43] and interact with other glycolytic enzymes [44]. For the first time, our findings revealed that NQO1 can bind to PKLR (Fig. 6) and trigger signal transduction in BC cells, consequently activating the AMPK and AKT/mTOR pathway and promoting cell motility capability.

Another study has suggested that NQO1 can enhance NSCLC cell proliferation by increasing cellular glycometabolism and HKII, which is a key regulator of this mechanism [6]. Some of our results are consistent with this finding, as we found that PKLR expression is regulated by NQO1 (Fig. 6). Interestingly, PKLR is thought to be a pivotal regulator of glycolytic reprogramming; for example, inhibition of PKLR activity leads to influenced anaerobic metabolism [45,46]. Nguyen et al. found that PKLR expression was increased in liver metastases as well as in primary colorectal tumors of patients with metastatic disease [47]. Nie et al. demonstrated that mineralocorticoid receptor (MR) inhibits the Warburg effect and cancer progression via the miR-338-3p-PKLR axis in HCC [48]. As expected, our findings revealed that PKLR knockdown clearly repressed proliferation, migration, and invasion by using siRNA in NQO1-overexpressing cells (Fig. 6). Consistent with these data, we also showed that knockdown of PKLR reversed NQO1-

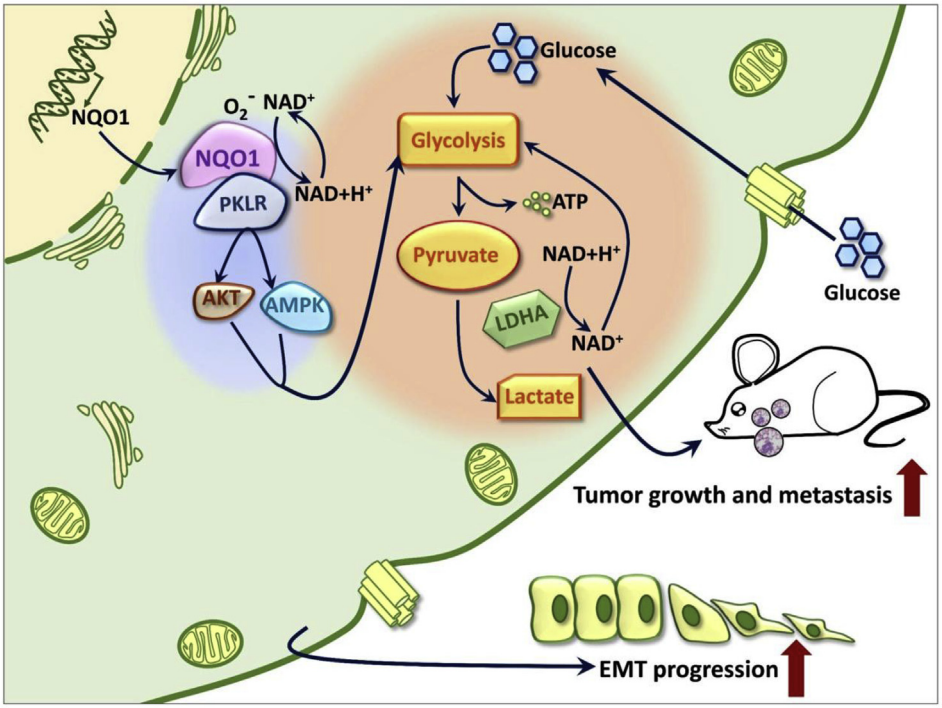

Fig. 8. Schematic model showing the role of NQO1 in the regulation of metastasis and glucose metabolism in BC.

mediated cellular glycolysis and EMT progression. Our findings suggest that PKLR is a downstream effector of NQO1 and regulates glucose metabolism in BC cells. Collectively, the results suggest that disrupting the NQO1/PKLR signaling axis may be effective in preventing primary tumor glycolysis and the EMT.

Our clinical study included 296 patients with early surgically resectable BC, analysis of this cohort indicated that high expression of NQO1 may be a prognostic biomarker and is closely related to LN metastasis. Similar results have been observed in HCC, suggesting that NQO1 plays an important role in cellular defense [35]. Our data observed that NQO1 is significant role for the activation of PKLR-related pathways in BC and that positive NQO1 and PKLR expressions are significantly associated with LN metastasis in BC (Tables 2 and 4). We also revealed that PKLR expression is higher in III-IV-stage BC than in 0-II-stage BC (Table 4), indicating that PKLR expression may facilitate NQO1-induced metastasis in late-stage disease. This link might also explain the higher incidence of lymph node metastasis in BC than in other types of cancer. In addition, patients with upregulated PKLR had a significantly shorter survival period than those with normal PKLR levels ($P < 0.00$) (Fig. 7F). Taken together, these data suggest that the NQO1/PKLR axis is associates with poor prognosis in BC patients, which indicates the possibility of targeting NQO1 and its downstream effectors as a therapeutic strategy.

In summary, the work presented here shows that NQO1 and PKLR are over-expressed in BC with LN metastasis and are well correlate with poor survival. NQO1 enhances BC cell proliferation and metastasis by modulating glycolytic reprogramming, providing the first evidence of an NQO1/PKLR network in BC (Fig. 8). These data indicates that NQO1/PKLR signaling may be an effective therapeutic target for BC treatment. However, further studies should be performed to identify the precise sites mediating the association between NQO1 and PKLR, which will be a key to developing specific inhibitors targeting NQO1/PKLR signaling.

Author contributions

YY and ZHL designed the study, YY and LYC provided technical support for CoIP and PCR array experiments. YY, GZ, JJP and ZHL participated in the tissue sample selection and experiments. YY, GZ and BD, performed experiments and analyzed data. YY, LYC and ZHL wrote the manuscript.

Conflicts of interest

The authors declare no financial conflict.

Acknowledgements

This study was supported by grants from National Natural Science Foundation of China (No. 31760313; No. 81660436), The Funds of Changbai Mountain Scholar Project and Key Laboratory of the Science and Technology Department of Jilin Province (No. 20170622007JC).

References

[1] S. Valastyan, R.A. Weinberg, Tumor metastasis: molecular insights and evolving paradigms, Cell 147 (2011) 275–292.
[2] I.J. Fidler, The pathogenesis of cancer metastasis: the 'seed and soil' hypothesis revisited, Nat. Rev. Canc. 3 (2003) 453–458.
[3] B. Weigelt, J.L. Peterse, L.J. van 't Veer, Breast cancer metastasis: markers and models, Nat. Rev. Canc. 5 (2005) [591]–[602] D.C. Wallace, Mitochondria and cancer, Nat. Rev. Canc. 12 (2012) 685-698.
[4] B. Yeo, N.C. Turner, A. Jones, An update on the medical management of breast cancer, BMJ 348 (2014) g3608.
[5] A. Lujambio, M. Esteller, How epigenetics can explain human metastasis: a new role for microRNAs, Cell Cycle 8 (2009) 377–382.
[6] Y. Cheng, J. Li, M. Martinka, G. Li, The expression of NAD(P)H: quinone oxidoreductase 1 is increased along with NF-kappaB p105/p50 in human cutaneous melanomas, Oncoogyl. Rep. 23 (2010) 973–979.
[7] M. Igarashi, B.R. Alford, Y. Nakai, W.P. Gordon, Behavioral auditory function after transection of crossed olivo-cochlear bundle in the cat. I. Pure-tone threshold and perceptual signal-to-noise ratio, Acta. Otolaryngolica 73 (1972) 455–466.
[8] D. Siegel, C. Yan, D. Ross, NAD(P)H:quinone oxidoreductase 1 (NQO1) in the sensitivity and resistance to antitumor quinines, Biochem. Pharmacol. 83 (2012) 1033–1040.
[9] D. Ross, D. Siegel, NAD(P)H:quinone oxidoreductase 1 (NQO1, DT-diaphorase), functions and pharmacogenetics, Methods Enzymol. 382 (2004) 115–144.
[10] Y. Yang, Y. Zhang, Q. Wu, X. Cui, Z. Lin, S. Liu, Y. Chen, Clinical implications of high NQO1 expression in breast cancers, J. Exp. Clin. Cancer Res. 33 (2014) 14.
[11] X. Cui, L. Li, G. Yan, K. Meng, Z. Lin, Y. Nan, G. Jin, C. Li, High expression of NQO1

is associated with poor prognosis in serous ovarian carcinoma, BMC Canc. 15 (2015) 244.
[12] Y. Ma, J. Kong, G. Yan, X. Ren, D. Jin, T. Jin, Z. Lin, NQO1 overexpression is associated with poor prognosis in squamous cell carcinoma of the uterine cervix, BMC Canc. 14 (2014) 414.
[13] X. Zhang, K. Han, D.H. Yuan, C.Y. Meng, Overexpression of NAD(P)H: quinone oxidoreductase 1 inhibits hepatocellular carcinoma cell proliferation and induced apoptosis by activating AMPK/PGC-1α pathway, DNA Cell Biol. 36 (2017) 256–263.
[14] X. Cheng, F. Liu, H. Liu, G. Wang, H. Hao, Enhanced glycometabolism as a mechanism of NQO1 potentiated growth of NSCLC revealed by metabolomic profiling, Biochem. Biophys. Res. Commun. 496 (2018) 31–36.
[15] D. Hanahan, R.A. Weinberg, Hallmarks of cancer: the next generation, Cell 144 (2011) 646–674.
[16] R.K. Tekade, X. Sun, The Warburg effect and glucose-derived cancer theranostics, Drug Discov. Today 22 (2017) 1637–1653.
[17] Z. Chen, X. Zuo, Y. Zhang, G. Han, L. Zhang, J. Wu, X. Wang, MiR-3662 suppresses hepatocellular carcinoma growth through inhibition of HIF-1α-mediated Warburg effect, Cell Death Dis. 9 (2018) 549.
[18] O. WARBURG, On the origin of cancer cells, Science 123 (1956) 309–314.
[19] S.A. Salama, M.A. Mohammad, C.R. Diaz-Arrastia, M.W. Kamel, G.S. Kilic, B.T. Ndofor, M.S. Abdel-Baki, Estradiol-17β upregulates pyruvate kinase M2 expression to coactivate estrogen receptor-α and to integrate metabolic reprogramming with the mitogenic response in endometrial cells, J. Clin. Endocrinol. Metab. 99 (2014) 3790–3799.
[20] P. Szyniarowski, E. Corcelle-Termeau, T. Farkas, M. Høyer-Hansen, J. Nylandsted, T. Kallunki, A comprehensive siRNA screen for kinases that suppress macroautophagy in optimal growth conditions, Autophagy 7 (2011) 892–903.
[21] S.L. Locatelli, G. Careddu, S. Serio, F.M. Consonni, A. Maeda, S. Viswanadha, S. Vakkalanka, L. Castagna, A. Santoro, P. Allavena, A. Sica, C. Carlo-Stella, Targeting cancer cells and tumor microenvironment in preclinical and clinical models of Hodgkin lymphoma using the dual PI3Kδ/γ inhibitor RP6530, 2018 Oct 23. pii: clincanres.1133, Clin. Cancer Res. (2018), https://doi.org/10.1158/1078-0432. CCR-18-1133 [Epub ahead of print].
[22] H.R. Christofk, M.G. Vander, Heiden, M.H. Harris, A. Ramanathan, R.E. Gerszten, R. Wei, M.D. Fleming, S.L. Schreiber, L.C. Cantley, The M2 splice isoform of pyruvate kinase is important for cancer metabolism and tumour growth, Nature 452 (2008) 230–233.
[23] Z. Lin, M. Bazzaro, M.C. Wang, K.C. Chan, S. Peng, R.B. Roden, Combination of proteasome and HDAC inhibitors for uterine cervical cancer treatment, Clin. Cancer Res. 15 (2009) 570–577 2009.
[24] M. Guarino, B. Rubino, G. Ballabio, The role of epithelial-mesenchymal transition in cancer pathology, Pathology 39 (2007) 305–318.
[25] Y.H. Cha, J.I. Yook, H.S. Kim, N.H. Kim, Catabolic metabolism during cancer EMT, Arch Pharm. Res. (Seoul) 38 (2015) 313–320.
[26] Y.X. Lu, H.Q. Ju, Z.X. Liu, D.L. Chen, Y. Wang, Q. Zhao, Q.N. Wu, Z.L. Zeng, H.B. Qiu, P.S. Hu, Z.Q. Wang, D.S. Zhang, F. Wang, R.H. Xu, ME1 regulates NADPH homeostasis to promote gastric cancer growth and metastasis, Cancer Res. 78 (2018) 1972–1985.
[27] P. Jiang, W. Du, A. Mancuso, K.E. Wellen, X. Yang, Reciprocal regulation of p53 and malic enzymes modulates metabolism and senescence, Nature 493 (2013) 689–693.
[28] J. Fan, J. Ye, J.J. Kamphorst, T. Shlomi, C.B. Thompson, J.D. Rabinowitz, Quantitative flux analysis reveals folate-dependent NADPH production, Nature 510 (2014) 298–302.
[29] R. Huang, X. Zong, Aberrant cancer metabolism in epithelial-mesenchymal transition and cancer metastasis: mechanisms in cancer progression, Crit. Rev. Oncol. Hematol. 115 (2017) 13–22.
[30] K. Kinslechner, D. Schörghofer, B. Schütz, M. Vallianou, B. Wingelhofer, W. Mikulits, C. Röhrl, M. Hengstschläger, R. Moriggl, H. Stang, M. Mikula, Malignant phenotypes in metastatic melanoma are governed by SR-BI and its association with glycosylation and STAT5 activation, Mol. Canc. Res. 16 (2018) 135–146.
[31] Y. Zhang, Y. Fan, S. Huang, G. Wang, R. Han, F. Lei, A. Luo, X. Jing, L. Zhao, S. Gu, X. Zhao, Thymoquinone inhibits the metastasis of renal cell cancer cells by inducing autophagy via AMPK/mTOR signaling pathway, Cancer Sci. 109 (2018) 3865–3873.
[32] Z. Yang, H. Xie, D. He, L. Li, Infiltrating macrophages increase RCC epithelial mesenchymal transition (EMT) and stem cell-like populations via AKT and mTOR signaling, Oncotarget 7 (2016) 44478–44491.
[33] D. Jiao, J. Wang, W. Lu, X. Tang, J. Chen, H. Mou, Q.Y. Chen, Curcumin inhibited HGF-induced EMT and angiogenesis through regulating c-Met dependent PI3K/Akt/mTOR signaling pathways in lung cancer, Mol. Ther. Oncolytics. 3 (2016) 16018.
[34] A. Strassburg, C.P. Strassburg, M.P. Manns, R.H. Tukey, Differential gene expression of NAD(P)H:quinone oxidoreductase and NRH:quinone oxidoreductase in human hepatocellular and biliary tissue, Mol. Pharmacol. 61 (2002) 320–325.
[35] L. Lin, J. Sun, Y. Tan, Z. Li, F. Kong, Y. Shen, C. Liu, L. Chen, Prognostic implication of NQO1 overexpression in hepatocellular carcinoma, Hum. Pathol. 69 (2017) 31–37.
[36] Y. Yang, X. Zhou, M. Xu, J. Piao, Y. Zhang, Z. Lin, L. Chen, β-lapachone suppresses tumour progression by inhibiting epithelial-to-mesenchymal transition in NQO1-positive breast cancers, Sci. Rep. 7 (2017) 2681.
[37] L. Cao, L.S. Li, C. Spruell, L. Xiao, G. Chakrabarti, E.A. Bey, K.E. Reinicke, M.C. Srougi, Z. Moore, Y. Dong, P. Vo, W. Kabbani, C.R. Yang, X. Wang, F. Fattah, J.C. Morales, E.A. Motea, W.G. Bornmann, J.S. Yordy, D.A. Boothman, Tumor-selective, futile redox cycle-induced bystander effects elicited by NQO1 bioactivatable radiosensitizing drugs in triple-negative breast cancers, Antioxidants Redox Signal. 21 (2014) 237–250.
[38] G. Chakrabarti, M.A. Silvers, M. Ilcheva, Y. Liu, Z.R. Moore, X. Luo, J. Gao, G. Anderson, L. Liu, V. Sarode, D.E. Gerber, S. Burma, R.J. DeBerardinis, S.L. Gerson, D.A. Boothman, Tumor-selective use of DNA base excision repair inhibition in pancreatic cancer using the NQO1 bioactivatable drug, β-lapachone, Sci. Rep. 5 (2015) 17066.
[39] K.R. Katikireddy, T.L. White, T. Miyajima, S. Vasanth, D. Raoof, Y. Chen, M.O. Price, F.W. Price, U.V. Jurkunas, NQO1 downregulation potentiates menadione-induced endothelial-mesenchymal transition during rosette formation in Fuchs endothelial corneal dystrophy, Free Radic. Biol. Med. 116 (2018) 19–30.
[40] L. Schwartz, T. Seyfried, K.O. Alfarouk, J. Veiga Moreira Da, S. Fais, Out of Warburg effect: an effective cancer treatment targeting the tumor specific metabolism and dysregulated pH, Semin. Canc. Biol. 43 (2017) 134–138.
[41] G.F. Weber, Metabolism in cancer metastasis, Int. J. Cancer 1 (2016) 2061–2066.
[42] S.O. Lim, C.W. Li, W. Xia, H.H. Lee, S.S. Chang, J. Shen, J.L. Hsu, D. Raftery, D. Djukovic, H. Gu, W.C. Chang, H.L. Wang, M.L. Chen, L. Huo, C.H. Chen, Y. Wu, A. Sahin, S.M. Hanash, G.N. Hortobagyi, M.C. Hung, EGFR signaling enhances aerobic glycolysis in triple-negative breast cancer cells to promote tumor growth and immune escape, Cancer Res. 7 (2016) 1284–1296.
[43] A.L. Hillis, A.N. Lau, C.X. Devoe, T.L. Dayton, L.V. Danai, D. Di Vizio, M.G. Vander Heiden, PKM2 is not required for pancreatic ductal adenocarcinoma, Cancer Metabol. 7 (2016) 1284–1296.
[44] R. Fang, T. Xiao, Z. Fang, Y. Sun, F. Li, Y. Gao, Y. Feng, L. Li, Y. Wang, X. Liu, H. Chen, X.Y. Liu, H. Ji, MicroRNA-143 (miR-143) regulates cancer glycolysis via targeting hex okinase 2 gene, J. Biol. Chem. 287 (2012) 23227–23235.
[45] M. Laplante, D.M. Sabatini, mTOR signaling in growth control and disease, Cell 149 (2012) 274–293.
[46] A. Cavazzoni, M.A. Bonelli, C. Fumarola, S. La Monica, K. Airoud, R. Bertoni, R.R. Alfieri, M. Galetti, S. Tramonti, E. Galvani, A.L. Harris, L.A. Martin, D. Andreis, A. Bottini, D. Generali, P.G. Petronini, Overcoming acquired resistance to letrozole by targeting the PI3K/AKT/mTOR pathway in breast cancer cell clones, Cancer Lett. 323 (2012) 77–87.
[47] A. Nguyen, J.M. Loo, R. Mital, E.M. Weinberg, F.Y. Man, Z. Zeng, P.B. Paty, L. Saltz, Y.Y. Janjigian, E. de Stanchina, S.F. Tavazoie, PKLR promotes colorectal cancer liver colonization through induction of glutathione synthesis, J. Clin. Investig. 126 (2016) 681–694.
[48] H. Nie, J. Li, X.M. Yang, Q.Z. Cao, M.X. Feng, F. Xue, L. Wei, W. Qin, J. Gu, Q. Xia, Z.G. Zhang, Mineralocorticoid receptor suppresses cancer progression and the Warburg effect by modulating the miR-338-3p-PKLR axis in hepatocellular carcinoma, Hepatology 62 (2015) 1145–1159.